

THE SUMMER HEMISPHERE HADLEY CELL

by

LLOYD L. SCHULMAN

B. S. , University of Michigan
(1970)

SUBMITTED IN PARTIAL FULFILLMENT OF THE
REQUIREMENTS FOR THE DEGREE OF
MASTER OF SCIENCE
at the
MASSACHUSETTS INSTITUTE OF TECHNOLOGY

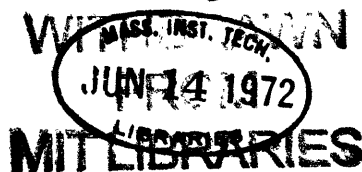
March, 1972

Signature of Author.....
Department of Meteorology, 21 March 1972

Certified by.....
Thesis Supervisor

Accepted by.....
Chairman, Departmental Committee on
Graduate Students

Lindgren



THE SUMMER HEMISPHERE HADLEY CELL

BY

LLOYD L. SCHULMAN

Submitted to the Department of Meteorology on 21 March 1972
in partial fulfillment of the requirements for the degree of
Master of Science.

ABSTRACT

In the extreme seasons the winter hemisphere Hadley cell dominates the entire zonally averaged mean meridional circulation by extending well into the summer hemisphere, and the summer hemisphere Hadley cell practically disappears. The hypothesis that this apparent disappearance is due to the process of zonal averaging, and that a summer hemisphere Hadley cell does exist when the averaging is restricted to the longitudes not influenced by the Asiatic monsoon, is tested. Using data for 1957-1964 covering the months June-August, it was found that the summer hemisphere Hadley cell was indeed present over the longitudes 160E-0-30E, or two thirds of the tropics.

A detailed error analysis, constituting the bulk of this thesis, is presented and the results are shown to be at least qualitatively correct. It is argued that the most interesting features of the meridional circulation and their associated transport processes are obscured by the zonal averaging process.

Thesis Supervisor: Edward N. Lorenz
Title: Professor of Meteorology

Table of Contents

1. Introduction	5
1.1 Background	5
1.2 Statement of Hypothesis	7
1.3 The Monsoon	8
2. Data	9
3. The Meridional Circulation for June-August	13
3.1 Zonally Averaged	13
3.2 Non-Zonal Longitudinal Averaging	18
4. Error Analysis	22
4.1 Previous Error Estimates	22
4.2 Standard Error of \overline{v}	26
4.21 Basis for Error Analysis	26
4.22 Formulation	27
4.23 Analysis	31
4.24 Results	35
5. Conclusions and Implications	39
References	42
Acknowledgements	44

List of Figures

Figure 1.3	ITCZ and surface wind observations for July (after Das, 1968)	10
Figure 2	Location of stations used in this study	11
Figure 3.1(a)	Zonally averaged meridional velocities for June-August	15
Figure 3.1(b)	Mass streamlines for June-August (after Newell et al., 1972)	16
Figure 3.1(c)	Mass streamlines for June-August (after Kidson et al., 1969)	17
Figure 3.2(a)	Averaged meridional velocities for 40E-150E for June-August	19
Figure 3.2(b)	Averaged meridional velocities for 160E-0-30E for June-August	20

List of Tables

Table I	Error analysis results for 200 mb, 30N	38
---------	--	----

1. Introduction

1.1. Background

Since the publication of Hadley's (1735) famous paper on the cause of the trade winds, the structure of the mean meridional circulation has been the source of much debate. It was not, however, until the advent of a sufficiently dense network of upper-level observations after World War II that an adequate direct study of this circulation was possible. This thesis will be another contribution to this continuing study.

The mean meridional circulation is a long term zonal average of the northward component of the wind and its corresponding vertical motion over a period of several months or years. Annually averaged, it usually consists of three distinct cellular motions in each hemisphere. The direct cell in low latitudes, where warm air rises near the equator and cooler air sinks near 30° , is called a Hadley cell. In mid-latitudes an indirect circulation known as the Ferrel cell exists. At the higher latitude evidence indicates the presence of a weak polar direct cell.

The mean meridional circulation can be estimated by two basic techniques. The first and most obvious is by direct observation. Surface and upper-level measurements of the meridional component of the wind, V , are averaged over time and space to form the quantity $[\bar{V}]$ at different latitudes and pressure levels, where the bar represents a time average and the brackets represent a zonal average around the latitude circle. After applying a correction to the meridional velocities which ensures a zero net mass flow through the latitude walls, the equa-

tion of continuity can be used to compute the streamlines of mass flow representing the mean meridional circulation:

$$2\pi a \cos\phi [\bar{v}] = g \frac{2\psi}{\partial p}$$

where a is the mean radius of the earth, ϕ is the latitude, g is gravity, p is pressure and ψ is the stream function.

The second technique uses indirect methods. In any given volume of the atmosphere over the long term there must be no net gain or loss of absolute angular momentum or of energy. Therefore the eddy transports of angular momentum or of energy must be balanced by friction, heating, or by a meridional cell transport. Our uncertain knowledge of the global heating distribution usually dictates the use of the angular momentum balance instead of energy. The most reliable procedure, outlined by Lorenz (1967) is to neglect the transport of angular momentum by the vertical eddies and, except in the layers below about 850 mb, to neglect frictional transfers. If the horizontal eddy momentum transport is known from wind measurements, then the mean meridional circulation needed to maintain the balance can be deduced. In the friction layer below 850 mb, the mass streamlines are deduced from mass continuity.

The indirect method is most widely used in the middle and upper latitudes where the values of $[\bar{v}]$ are smaller and less well known than tropical values, and thus yields more acceptable results. The procedure breaks down near the equator. This study will basically be concerned with the Hadley cell, which is found in low latitudes, and

hence we will use the first technique of direct observation.

1.2. Statement of Hypothesis

From the previous observational studies of Kidson, Vincent and Newell (1969), Starr, Peixoto and Gaut (1970) and Oort and Rasmusson (1970), in addition to many pioneering studies, the three cell meridional circulation has been well established. In the spring and fall seasons as well as the annual mean, well developed Hadley and Ferrel cells exist in both hemispheres and are generally symmetrical about the equator. However, in the extreme seasons the winter hemisphere Hadley cell dominates the entire mean meridional circulation by extending well into the summer hemisphere, and the summer hemisphere Hadley cell practically vanishes.

Lorenz (1970) has proposed that the apparent disappearance of the summer hemisphere Hadley cell is merely due to the process of zonal averaging. During the extreme seasons an intense monsoonal circulation covers much of the south Asian continent and surrounding waters, with a strong inflow from deep within the winter hemisphere to deep within the summer hemisphere at low levels and a return outflow at higher levels. Lorenz contends that if a symmetrical Hadley and Ferrel cell pattern, such as in the spring and fall seasons, does exist also in the extreme seasons over, say, $2/3$ of the longitudes, with the Asiatic monsoon occupying the remaining longitudes, then the resulting zonal average of the two features would be precisely what is observed;

a more intense winter hemisphere Hadley cell and the elimination of the summer hemisphere Hadley cell.

If this circulation pattern is indeed the case, then by expressing the meridional circulation in terms of zonal averages, and ignoring the longitudinal asymmetries, we may be obscuring the prevailing circulation of the tropics. This thesis will be an attempt to verify this hypothesis by establishing the existence of a symmetrical Hadley cell pattern in the extreme seasons when the averaging is restricted to the regions of the tropics not influenced by the Asiatic monsoon.

1.3. The Monsoon

Before proceeding to the processing of data, the boundaries of the two longitudinal sectors to be used in the non-zonal averaging, namely the monsoonal longitudes and the remaining two thirds of the globe which we hypothesize as containing our symmetrical Hadley cell pattern, and the summer hemisphere to be examined must be decided upon. These can only be determined by a brief look at the Asiatic monsoon.

Monsoons are most pronounced in the summer season of either hemisphere, and since they are largely confined to the tropics, they may be thought of as the penetration of the trade winds from one hemisphere into the other, and bounded by the position of the intertropical convergence zone (ITCZ). The most intense and deeply penetrating one is the Asiatic monsoon during the northern hemisphere summer, which extends well into the northern hemisphere towards India, southeast Asia, and the east coast

of Africa. This can be readily seen from the plot of the ITCZ and the mean surface wind circulation for the month of July in Figure 1.3. During the northern hemisphere winter the direction of the Asiatic monsoon in these regions is reversed.

Because of the greater intensity and penetration of the Asiatic monsoon during the northern hemisphere summer, and also because of the denser observational network available in the northern hemisphere, this thesis will confine its attempt to verify the existence of the symmetrical Hadley cell pattern over much of the tropics in the extreme seasons to the northern hemisphere summer months of June-August. For the remaining case of the southern hemisphere summer, or December-February, a similar procedure could be followed.

A careful examination of Figure 1.3 also shows that the greatest monsoonal influence or northward penetration occurs between 40°E and 150°E longitude. These then will be used as the boundaries of the two longitudinal sectors in the non-zonal averaging process of Chapter 3.2.

2. Data

A detailed explanation of the data and its sources can be found in Chapter 2 of Newell, Kidson, Vincent and Boer (1972). As a brief summary, the results of this thesis have been based on the directly observed values of the meridional component of the wind, V , from 330 radiosonde and radar wind stations for the overall period July 1957 to

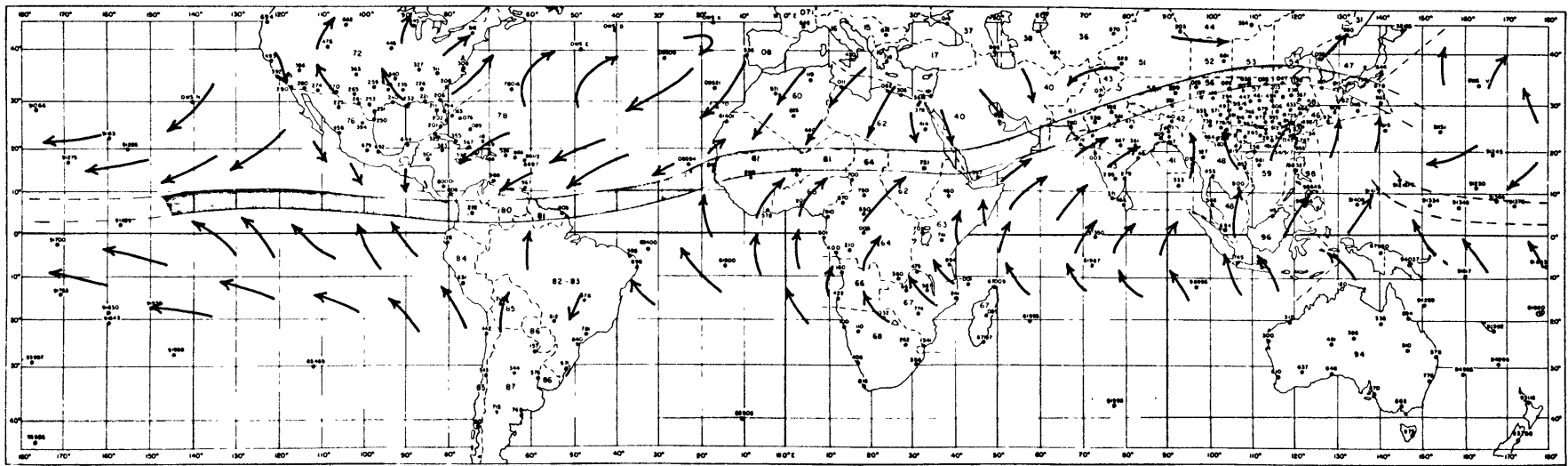


Figure 1.3

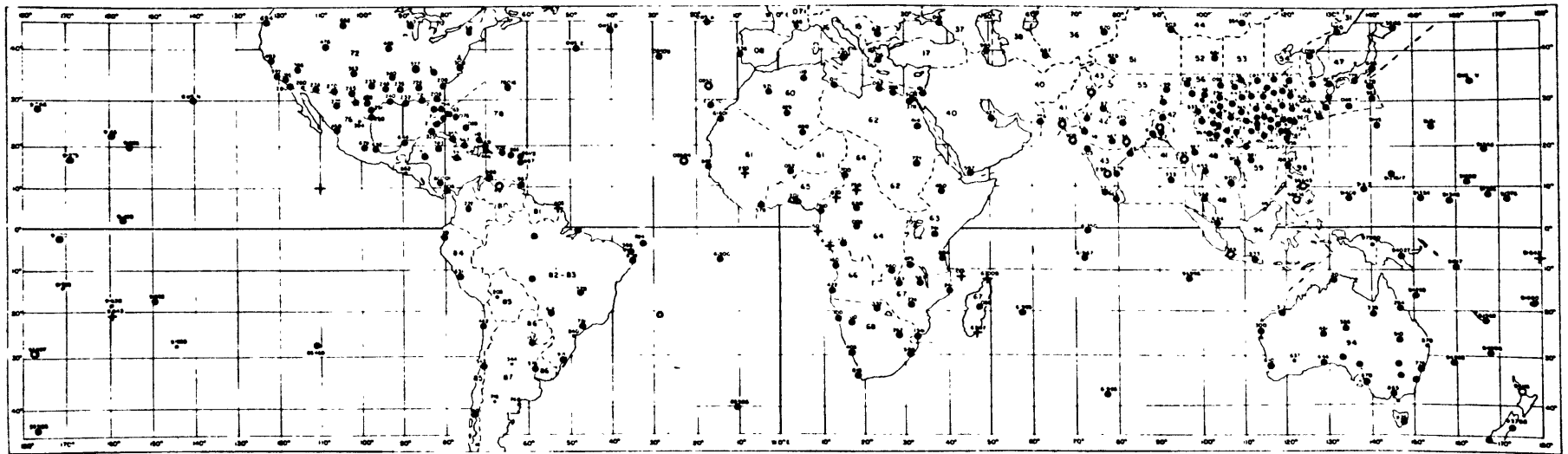


Figure 2

December 1964, covering an area from 45N to 45S latitude. Figure 2 shows the location of the stations.

Daily data for most of the northern hemisphere stations were supplied by the National Weather Records Center (NWRC) at Asheville, North Carolina. Much of this data was a part of the MIT General Circulation Data Library which was the result of V. P. Starr's five year (May 1958-April 1963) northern hemisphere study.

In the southern hemisphere approximately one fifth of the stations were also supplied by NWRC, but most of the station data was obtained from the Australian, Brazilian, British, French, New Zealand, and South African Meteorological Services.

Data from stations making only pilot balloon observations were not used because of the poor coverage at higher levels in the troposphere, and the resulting bias in favor of light winds and fair weather. Many stations did not report regularly throughout the period, causing a considerable variation in quality and quantity of the data between stations.

The principal reporting time was 0000 GMT but where necessary, data at 0600 and 1200 GMT were included to improve the coverage. The nine standard levels of 1000, 850, 700, 500, 400, 300, 200, 150, and 100 millibars were used. At each of these levels values of the long term mean meridional wind, \bar{V} , were plotted at the stations and subjectively analyzed for the four seasons; December-February, March-May, June-August, and September-November. The gridpoint values of \bar{V} were then read from the subjectively analyzed maps at 10 degree intervals of latitude

and 10 degree intervals of longitude for the region 40N-40S latitude. Station values of \bar{V} calculated from fewer than 30 observations were given little weight in the hand analysis.

3. The Meridional Circulation for June-August

3.1. Zonally Averaged

As a basis for comparison with the non-zonal longitudinal averaging in Chapter 3.2 of the regions 40E-150E and 160E-0-30E, this section will briefly review the results of the zonally averaged mean meridional circulation.

Figure 3.1(a) is a plot of the values of $[\bar{V}]$ for the months June-August from the 8 years of data. The dashed lines represent the approximate cell boundaries, and the arrow lengths are proportional to the wind speed. It can be clearly seen that the winter hemisphere Hadley cell dominates the mean circulation of the northern hemisphere. Mean meridional velocities of up to 2 m/sec can be observed in the lower branch of the Hadley cell and an even stronger return flow of over 3 m/sec is found in the upper branch at 200 mb. Between 700 mb and 300 mb the mean meridional velocities are generally less than 1 m/sec.

In the mid-latitudes of the southern hemisphere a well defined Ferrel cell circulation exists with lower branch velocities of 1 m/sec and upper branch velocities of over 3 m/sec. In contrast, the mean meridional velocities of the middle latitudes of the northern hemisphere in June-August

are weak and ill-defined.

A further evaluation of the cell structure can be made by examining the mass streamlines of the circulation, which can be calculated from these meridional velocities or the horizontal eddy momentum transports using the methods described in Chapter 1.1. This has already been done for these data by Newell et al. (1972), and the results are shown in Figure 3.1(b). The region from 20N to 20S was determined by the first technique of direct observation, and the remaining latitudes were indirectly deduced from angular momentum transport considerations. The intense winter hemisphere Hadley cell during June-August can be seen to extend from about 30S to 15N. All that remains of the summer hemisphere Hadley cell is a very weak direct circulation between 20N and 30N.

The same data was objectively analyzed by Kidson et al. (1969) and the mass streamlines, shown in Figure 3.1(c), were obtained by direct means. In this analysis the winter hemisphere Hadley cell during June-August also dominates the mean circulation pattern of the northern hemisphere, and occupies the latitudes 20S to 15N. The summer hemisphere Hadley cell is completely absent, with a very weak indirect circulation in its place.

In either case we can conclude that the zonally averaged summer hemisphere Hadley cell is of no consequence in the meridional circulation.

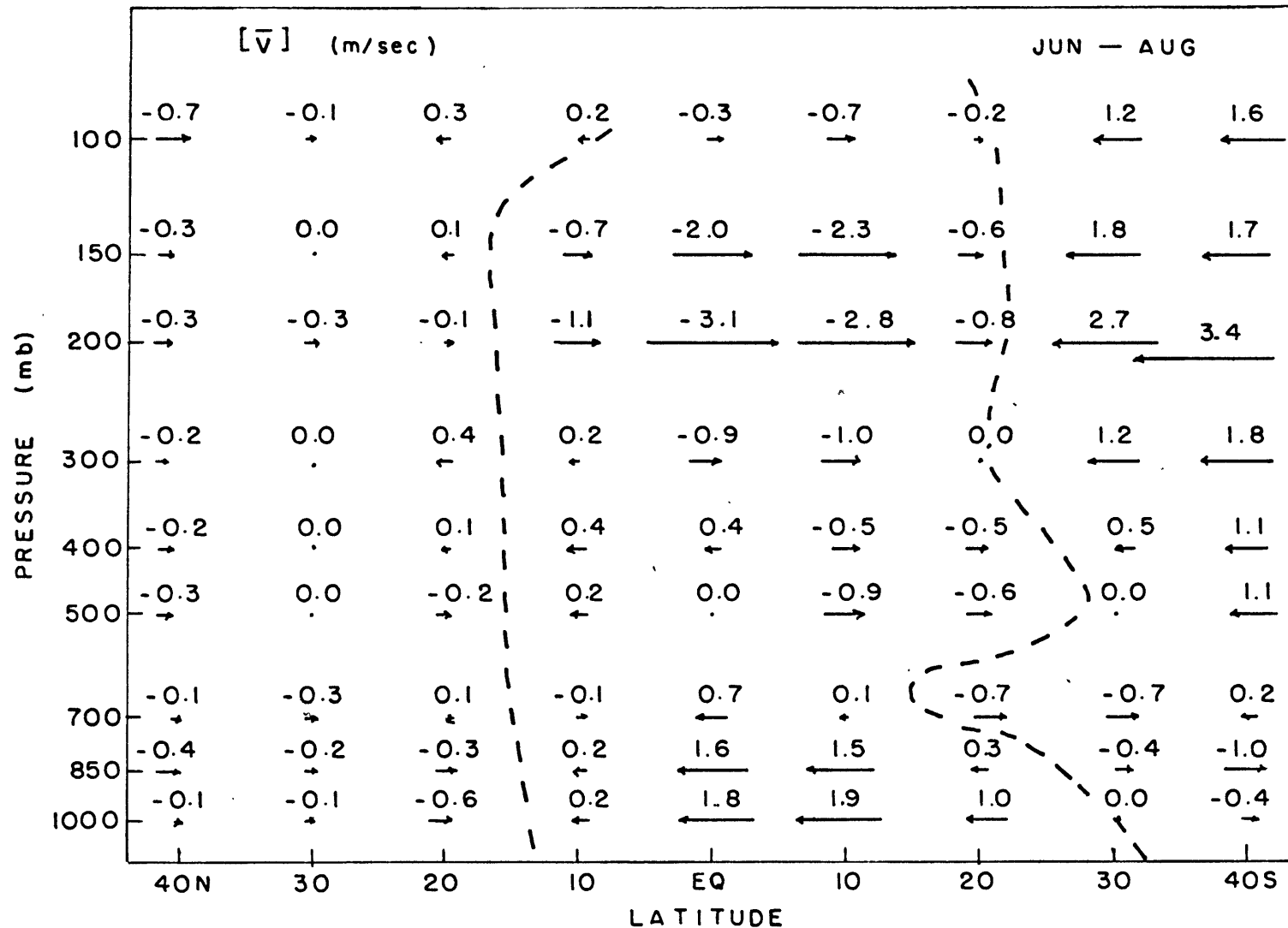


Fig. 3.1 (a) ZONALLY AVERAGED MERIDIONAL VELOCITIES

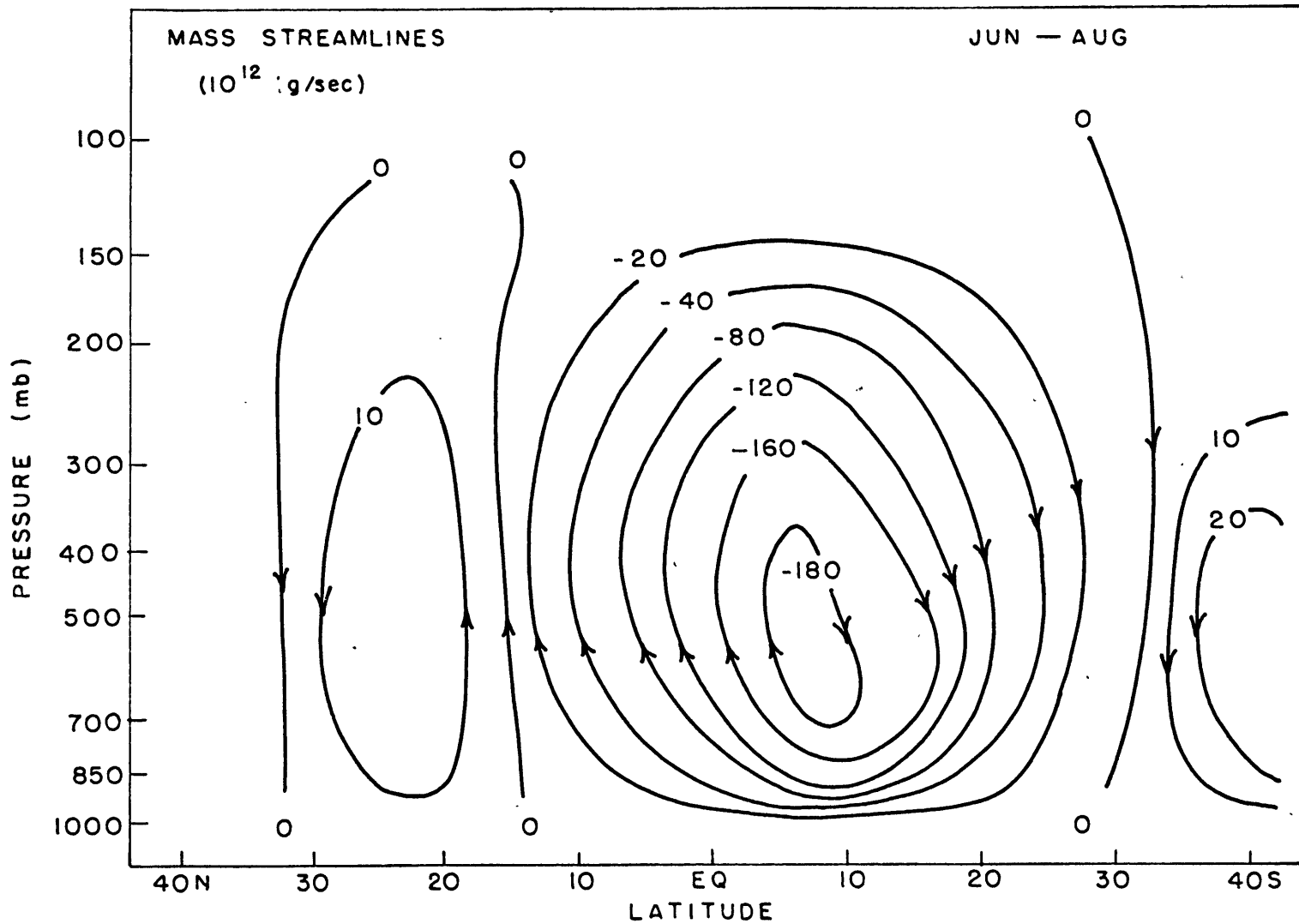


Fig. 3.1(b) ZONALLY AVERAGED CIRCULATION DETERMINED BY NEWELL ET AL (1972)

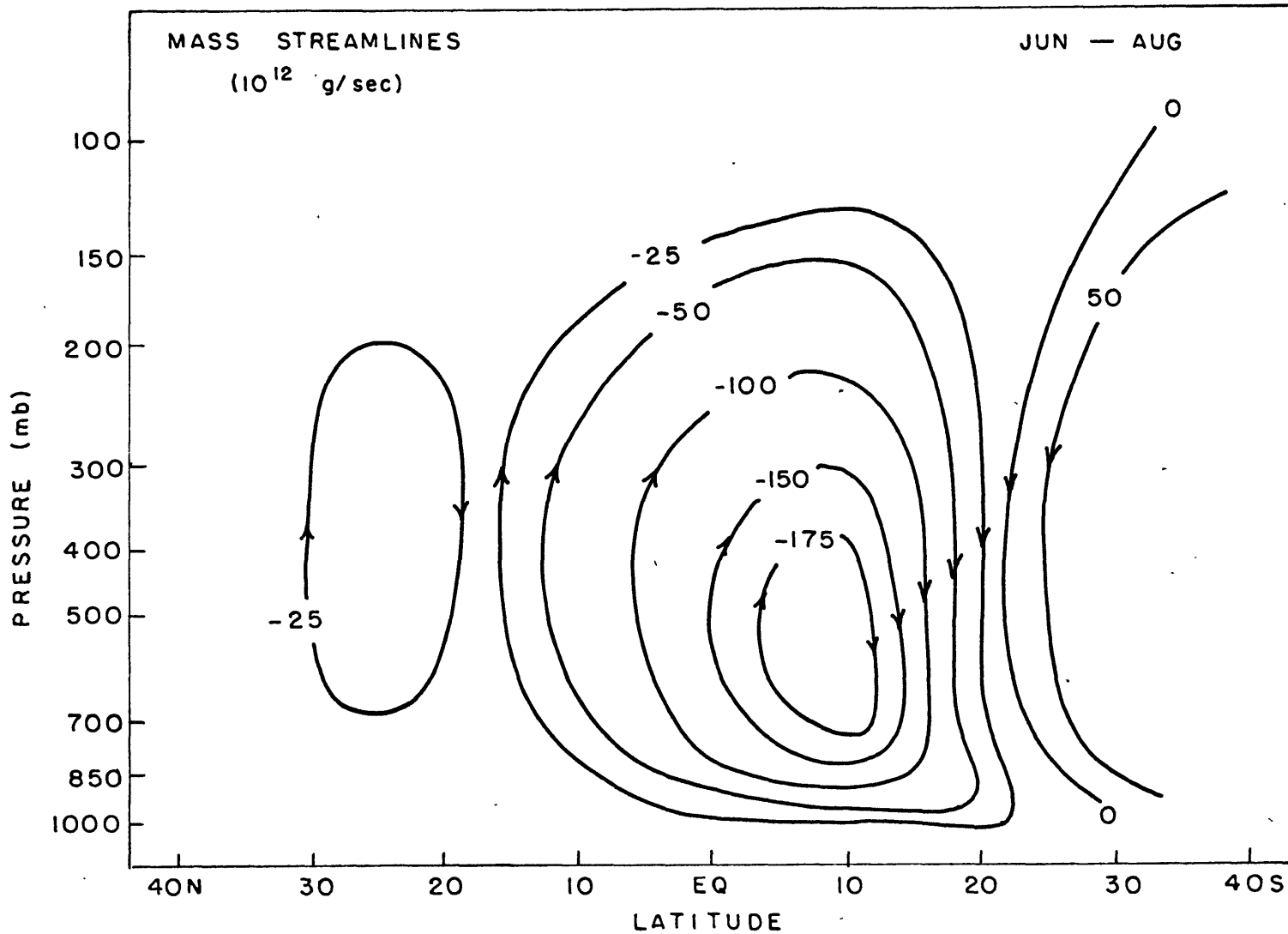


Fig. 3.1(c) ZONALLY AVERAGED CIRCULATION DETERMINED BY KIDSON
 ET AL (1969)

3.2. Non-Zonal Longitudinal Averaging

We can now separate our zonal average of the mean meridional circulation during June-August into the two components decided upon in Chapter 1.3; the longitudinal sector 40E -150E representing the region of monsoonal influence, and the remaining two thirds of the globe, 160E-0-30E, which we hypothesize as containing a symmetrical Hadley cell pattern. We will denote the averaged meridional circulation in these regions as $\{\bar{V}\}_{MON}$ and $\{\bar{V}\}_{HAD}$, respectively.

It should be noted that the errors inherent in the calculation of our meridional circulations have not been included in the figures that will be presented shortly. These errors and their effects upon our results will be considered in detail in Chapter 4, and will constitute the bulk of this thesis.

Figure 3.2(a) shows the results of averaging \bar{V} in the monsoon region only. Of immediate notice is the intensity and penetration of the Asiatic monsoon. The lower branch inflow extends from 30S to 30N and attains mean meridional velocities of over 3 m/sec. The upper branch return flow exhibits more strength, and extends from 40N to 25S with velocities approaching 5 m/sec. It is clearly a much more vigorous circulation than the winter hemisphere Hadley cell observed in Figure 3.1(a), and penetrates a full 15 degrees of latitude further into the northern hemisphere. The only other discernable feature appears in the southern hemisphere between 25S to 40S and is probably just the beginning of the Ferrel cell circulation appearing on the zonally averaged figures.

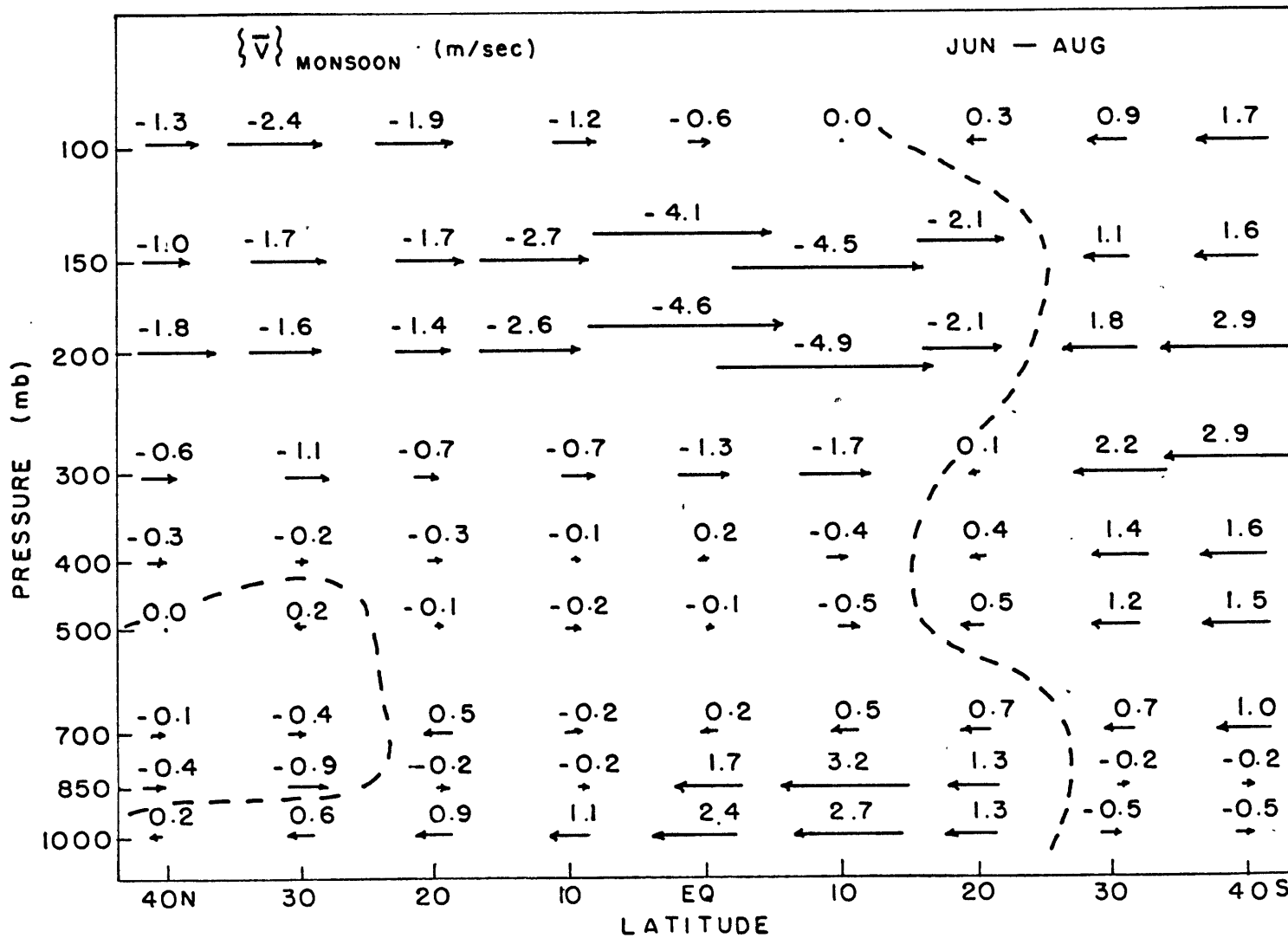


Fig. 3.2(d) AVERAGED MERIDIONAL VELOCITIES FOR 40°E - 150°E

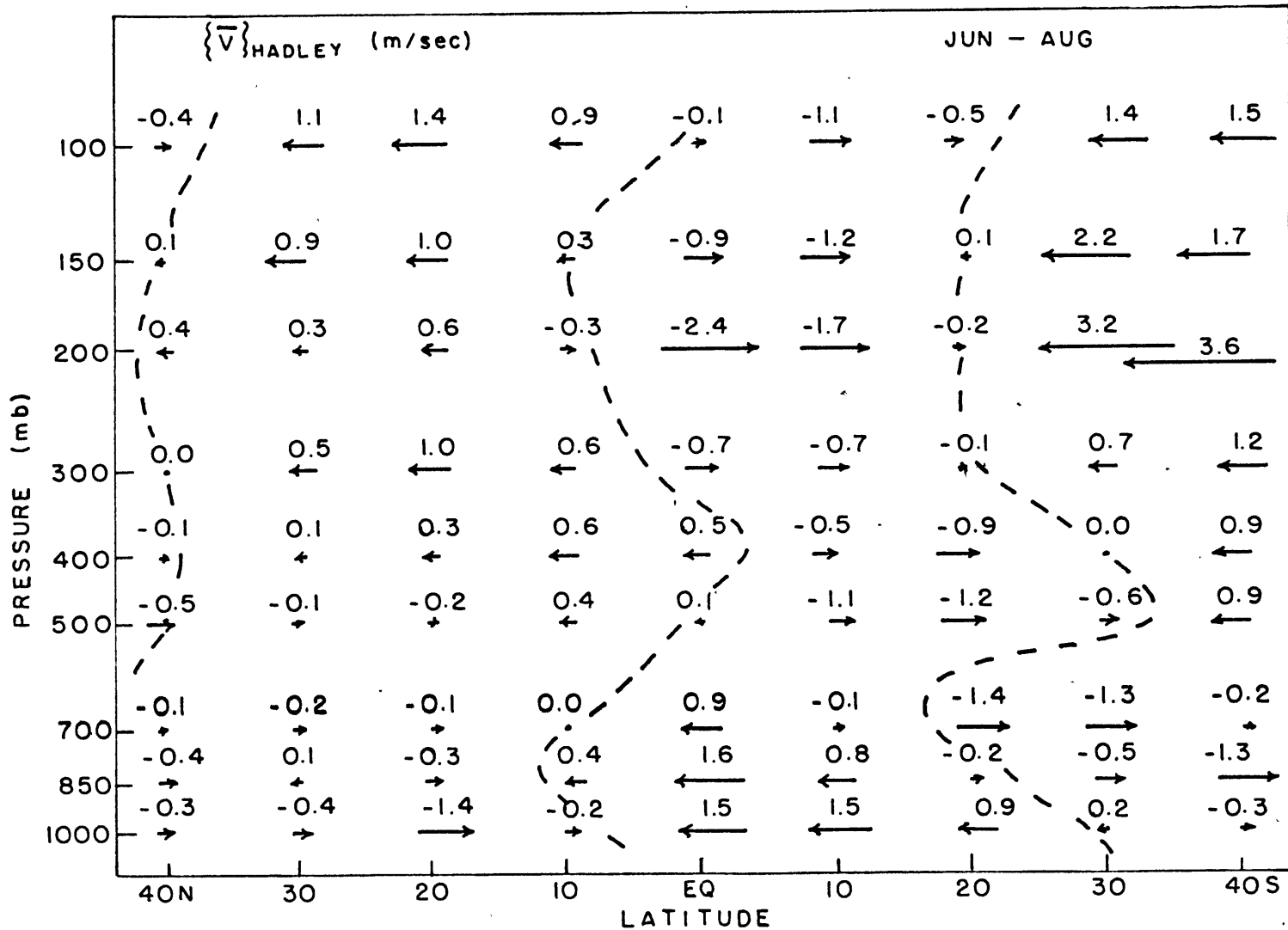


Fig. 3.2 (b) AVERAGED MERIDIONAL VELOCITIES FOR 160°E - 0° - 30°E

The results which are of crucial importance to this thesis are presented in Figure 3.2(b). It is a plot of \bar{V} during June-August averaged over the remaining longitudes of the globe, $\{\bar{V}\}_{HAD}$, and the resulting pattern represents the prevailing circulation of the tropics. We can see that it is almost a symmetric Hadley cell pattern as was hypothesized.

The winter hemisphere Hadley cell extends from about 25S to only 5 N, unlike the penetration to 15N of the zonally averaged cell in Figure 3.1(a). In addition, the intensity of the winter hemisphere Hadley cell in Figure 3.2(b) is substantially less than the zonally averaged cell of Figure 3.1(a). Meridional velocities in the lower branch are about 0.5 m/sec less, and the velocities of the upper branch have been reduced from about 3 m/sec to about 2 m/sec. Also in the southern hemisphere we can see a well defined Ferrel circulation which extends from about 25S to some point beyond 40S.

Most importantly of course is that a summer hemisphere Hadley cell is distinctly present, with a northward extent to somewhere beyond 30N. It does not appear, however, to be of equal strength with the winter hemisphere Hadley cell. Average meridional velocities in the upper branch are only as high as 1.4 m/sec, about 0.5 m/sec below those in the winter cell, but still are in much closer agreement with our hypothesized circulation than the small non-definitive velocities present in Figure 3.1(a) at these levels. The lower branch of the summer hemisphere Hadley cell is not as encouraging, with its many small velocities, but it does contain a meridional velocity of

1.4 m/sec, which is comparable with the velocities found in the winter cell.

It should be noted that unlike the zonally averaged circulation, mass streamlines of the averaged meridional circulation in these two longitudinal sectors cannot be calculated, since there is no assurance of mass conservation in the regions.

All of the averaged velocities thus far have been accepted without question. But when working with the mean meridional circulation the accuracy of the results must always be questioned. As was stated earlier, before we can conclude that the hypothesis has been verified, the errors in $[\bar{v}]$, $\{\bar{v}\}_{MON}$, and $\{\bar{v}\}_{HAD}$ must be computed. This will be done in the next chapter.

4. Error Analysis

4.1. Previous Error Estimates

The difficulty in determining the mean meridional motion from direct observations is well known, and can be readily seen from the different analysis of Figures 3.1(b) and 3.1(c). The mean meridional velocity, $[\bar{v}]$, is usually a small residue obtained from averaging relatively large velocities having opposite signs, and is often exceeded by the daily variations. It is therefore quite sensitive to observational sampling.

Before deriving an estimate of the errors contained in our computed values of $[\bar{v}]$, $\{\bar{v}\}_{MON}$ and $\{\bar{v}\}_{HAD}$, it might be of some interest to briefly review the efforts of previous investigators

to cope with the errors involved in $[\bar{v}]$ computations.

As pointed out in Starr et al. (1970), Oort and Rasmusson (1970), and Stoldt (1971), the vertical mass average of $[\bar{v}]$ namely $\frac{1}{p_0} \int_0^{p_0} [\bar{v}] d\rho$, should over the long term be very close to zero. It would therefore follow that an unbalanced net meridional circulation would be an indication of poor data and that the magnitude of the vertically averaged $[\bar{v}]$ could be used as a measure of its reliability. This precludes the possibility of canceling errors in the vertical average.

Two effects could be responsible for a non-zero value of the vertically averaged $[\bar{v}]$. The first is the seasonal mass shift or storage effect. During June-August there is a net mass flow into the northern hemisphere which can be seen by observing the change in the mean surface pressure of both hemispheres. This would imply a net northward meridional drift velocity. However, as pointed out by Gordon (1953), a mean meridional drift of only 5 mm/sec for 3 months would account for the seasonal pressure change of one or two millibars.

The second effect is that of topography or the difference in height of the grid points used in the calculations of $[\bar{v}]$. Assume, for example, that on the same latitude circle northerly flows consistently take place over grid points at high elevations and southerly flows occur near sea level. If there is no actual net mass flow across the latitude walls then calculations which disregard the topography would indicate a fictitious southward mass flow. This is simply because there is a greater mass flow possible over the regions with a larger vertical distance in the atmos-

pheric column. A correlation of the vertically averaged value of \bar{v} with the height of the grid points on a latitude circle is needed to compute the corrections. Rough calculations indicate that for consistent height differences of 40 mb perfectly correlated with opposing \bar{v} values of 2 m/sec a correction of only 4 cm/sec would be necessary.

Hence, we can conclude that the two effects are negligible and the vertically averaged value of $[\bar{v}]$ over the summer season should be nearly equal to zero. The values for the data used are presented below as calculated for the layer 1000-100 mb, since all but a small fraction of the mass flow occurs in this layer.

Latitude	40N	30	20	10	EQ	10	20	30	40S	
$\frac{1}{900} \int_{100}^{1000} [\bar{v}] dp$	-0.25	-0.15	-0.04	+0.02	+0.12	-0.25	-0.25	+0.29	+0.79	m/sec

If we used the above reliability criteria, the most accurate data should be in the region between 10S and 20N, since from Fig. 3.1(a) for the other latitudes the corrections are larger than many of the values of $[\bar{v}]$ at the different pressure levels.

Kidson (1968) used the objective analysis scheme of Eddy (1967) in obtaining his value of $[\bar{v}]$. Assuming a 90% reduction of variance in his predicted wind fields, he arrives at 95% confidence limits of ± 0.4 m/sec as his error for good data coverage, and about ± 1.3 m/sec for isolated or poor coverage. This means, in the case of good data coverage, that one can say with 95% confidence that his calculated values of $[\bar{v}]$ fall within ± 0.4 m/sec of their true value. Since any given latitude circle

contains both good and bad coverage, his overall error estimate would be somewhere in between.

Oort and Rasmusson (1970) estimated the total error variance of $[\bar{v}]$ as the sum of the computed variances in time and space of v . Assuming an infinite population of observations of v , he calculated 95% confidence limits near the equator of ± 0.5 m/sec and ± 0.2 m/sec at heights of 200 mb and 1000 mb respectively. He concluded that low latitude features are generally statistically significant with the estimates of the lower branch of the Hadley cell being the more reliable. In the middle and high latitudes, his calculated mean meridional velocities were smaller than his error limits and therefore much less reliable than low latitudes.

Walker (1969) studied the possibility of a land-sea bias in the observation network and concluded that a more symmetrical choice of observing stations around the globe resulted in a different and more accurate value of $[\bar{v}]$. The values of $[\bar{v}]$ were more negative with the biased grid than with the unbiased grid at both 700 mb and 300 mb, implying that if a tendency toward more northerly flow was not detected by a less dense observing network over Europe, then certainly the present scanty sampling of oceanic regions is not representative of the true values of \bar{v} . The only valid way of eliminating the bias, of course, would be to increase the observations over the oceans.

4.2. Standard Error of $[\bar{v}]$

4.21. Basis for Error Analysis

The final value of $[\bar{v}]$ which we obtain is only an estimate of the true $[\bar{v}]$ which would be obtained with perfect data. The value of \bar{v} is calculated from, at best, daily observations whereas a true value of \bar{v} represents an integral of v over time. Similarly, the zonal average assumes a linear interpolation of \bar{v} between grid points or stations, and the true zonal average is represented by a spatial integral around the latitude circle. Our data cover only 8 summer seasons, which may not represent a long term $[\bar{v}]$, but only a recent trend in a slow periodic oscillation. These considerations in obtaining a true $[\bar{v}]$ cannot be reckoned with, but we can certainly imagine an ideal $[\bar{v}]$ and estimate our error as the deviation from this value.

Consider an ideal $[\bar{v}]$ as that value calculated from eight summers of errorless daily wind observations taken at the grid points. We will not be concerned with long term trends, or spatial and temporal integrals, but only with the years 1957-1964 and linear interpolation in space and time.

With this basis for the error analysis 3 major errors become immediately obvious. First is the error in wind observations. Most of the wind observations are from radiosonde data which are notably unreliable in high winds at upper levels. In such situations the standard error of measurement, σ_m , can be as high as 30 m/sec when the observed wind speed is about 75 m/sec.

Secondly, an error is introduced from missing observations. An ideal value of \bar{v} would be obtained if all possible observations of v , approximately 700 for the 8 summer seasons, are averaged linearly. However, in most cases only 300-600 observations are available. As will be shown shortly, the error introduced by the missing data in the calculation of \bar{v} can be estimated by considering the standard deviation, σ_o , of the observations of v at the stations.

The third and most apparent error arises from the fact that except in rare instances the observing stations do not coincide with the grid points. Some standard error of analysis, σ_a , must be introduced in subjectively hand-analyzing the station values of \bar{v} to the grid points.

4.22 Formulation

A formulation of these errors into an expression for the standard error of $[\bar{v}]$, $\sigma_{[\bar{v}]}$, can be accomplished after considering the averaging technique used to obtain $[\bar{v}]$. The procedure is as follows:

1. Time average v at stations
2. Hand average \bar{v} to grid points
3. Average grid point values around latitude circles

The three errors can now be seen to enter as follows:

—————→ instrument error σ_m

—————→ missing data error

1. Time average

—————→ analysis error σ_a

2. Hand analyze \bar{V} to grid points
3. Zonal average

Assuming the instrument errors are uncorrelated from day to day and station to station the variance of \bar{V} at the stations due to instrument error is σ_m^2/N where N is the number of observations. After analyzing to grid points, which entails averaging the variance σ_m^2/N at neighboring stations, a zonal average of values at 36 independent grid points results in an instrument error variance for $[\bar{V}]$ of $\frac{1}{36}[\sigma_m^2/N]$, where $[\sigma_m^2/N]$ is the average value of σ_m^2/N at the 36 grid points.

The variance of \bar{V} at the stations due to incomplete observations can be expressed according to Spiegel (1961) as $\frac{\sigma_D^2}{N_e} \left(\frac{N_{pe} - N_e}{N_{pe} - 1} \right)$, where σ_D^2 is the variance of the observations at the station, N_{pe} is the population size of independent observations, and N_e is the number of independent observations. The choice for N_{pe} and N_e is unclear. A conservative estimate commonly used in meteorology would be to assume every third observation is independent, but for stations with only a few observations, the observations may be spaced far enough apart to be independent anyway. Taking this into account a crude approximation for the number of independent observations would be

$$N_e = \frac{N}{1 + 2(N/N_p)} \quad \text{and} \quad N_{pe} = \frac{N_p}{3}$$

where N is the actual number of observations at a station and N_p is the actual population size of observations. For large values of N approaching N_p , N_e is equal to the conservative estimate of every third observation, while for small values of N , N_e is almost equal to N . For

the data used in this study, $N_p = 736$. We will assume $N_{pe} = 250$ for simplifying the computations.

Notice that for a complete set of observations, i. e., no missing data, $N_{pe} = N_e$ and the error variance vanishes. For a small number of observations the eight year \bar{v} cannot be determined accurately and a large error variance results.

As with the instrument errors, station values of the variance of \bar{v} are then averaged to neighboring grid points and these 36 values are averaged together. However, the variances at the grid points may be spatially correlated around a latitude circle since certain grid points derive their variances from the same stations, providing observations at these stations are on the same days. We can estimate the number of independent grid points in the zonal average as M , a sum of the number of grid points in a region of high station density and the number of stations along the latitude circle in a region of low station density. We can now express the missing data variance for $[\bar{v}]$ as $\frac{1}{M} \left[\frac{\sigma_D^2}{N_e} \left(\frac{N_{pe} - N_e}{N_{pe} - 1} \right) \right]$.

The variance of \bar{v} at the grid points due to the subjective analysis error is σ_a^2 , and the average grid point value becomes $[\sigma_a^2]$. As in the missing data error, the analysis error is highly correlated around a latitude circle since, especially in regions with a low station density, interpolations of \bar{v} values to the grid points uses the same stations. Once again we estimate the number of independent grid points in the zonal average as M . The analysis error variance for $[\bar{v}]$ becomes $\frac{1}{M} [\sigma_a^2]$.

Further, if we assume the 3 errors to be independent of each other, and this seems reasonable, then the total variance of $[\bar{V}]$ due to the 3 errors becomes:

$$\sigma_{[\bar{V}]}^2 = \frac{1}{M} [\sigma_a^2] + \frac{1}{M} \left[\frac{\sigma_D^2}{N_e} \left(\frac{N_{pe} - N_e}{N_{pe} - 1} \right) \right] + \frac{1}{36} \left[\frac{\sigma_m^2}{N} \right]$$

The above expression, however, implicitly assumes that there are no systematic errors present, and we will briefly discuss this possibility.

The representation of σ_a^2 , discussed in the next section, eliminates, for the most part, in its derivation the possibility of any systematic errors. Similarly we can assume that the instruments used in the upper level wind calculations were properly calibrated so as to eliminate any systematic errors in σ_m^2 . The greatest possibility for systematic errors to enter would be in the variance of \bar{V} at the stations due to incomplete observations. This would occur if the days of missing observations exhibited a preference for either northerly or southerly winds. However, we see no obvious reason, nor any indication in the data, that this is indeed the case. Therefore we will assume for the remainder of the error analysis that the systematic errors, if they exist, are very small and can be neglected.

4.23. Analysis

σ_p^2 is a quantity which is directly evaluated from the wind observations at the stations, whereas σ_m^2 and σ_a^2 are more flexible quantities which are not directly obtainable, but must be estimated mathematically after making reasonable assumptions.

The instrument error can be estimated from a formula by de Jong (1958). The standard error in upper level wind calculations for radio direction finding or theodolite techniques of balloon tracking is:

$$\sigma_m = \frac{\sqrt{2}}{\tau h} \left[(d^2 + h^2)^2 m_\epsilon^2 + d^2 m_h^2 \right]^{1/2}$$

where:

τ = time interval of observations = 60 sec

m_ϵ = standard error of elevation angle whose

estimated maximum by Klein (1968) = 0.12° or

2×10^{-3} radians. Average $m_\epsilon = 0.10^\circ$ and

for a good optical theodolite, $m_\epsilon = 0.02^\circ$.

m_h = standard error in height measurement also estimated by Klein (1968) as $0.2\% h$

h = height of balloon above release point

d = downrange distance from release point

We wish to maximize the error estimates but at the same time keep them reasonable. From wind observations σ_D consistently reaches its maximum at 200 mb. If the winds increase with height to jet stream levels, then it can be seen that with little or no directional shear, σ_m will also reach a maximum at about 200 mb.

From observational experience, Professor F. Sanders of M.I.T. estimates that by 200 mb a realistic long term average value for d is about 30 km. Estimating the time of ascent for a standard 100 gm balloon to this level to be 45 minutes (Handbook of Instruments, 1961), this is equivalent to a vertical wind shear of about 50 knots. Assuming 200 mb represents a height of 39,000 ft. or 12 km, the value of σ_m becomes:

$$\sigma_m = \frac{1.4}{60 \text{ sec } 12 \text{ km}} \left[(900 + 144)^2 4 \times 10^{-6} + 900 (2.4 \times 10^{-2})^2 \right]^{1/2} \text{ km}^2$$

$$\sigma_m^2 \sim 16 \text{ m}^2/\text{sec}^2$$

For radar tracking, errors reduce considerably and de Jong's formulas estimate for a similar situation:

$$\sigma_m^2 \sim 2.5 \text{ m}^2/\text{sec}^2$$

The analysis error is the most difficult to estimate, but a formula derived by Gleeson (1961) appears to be mathematically sound and gives reasonable results. He assumes the distribution of the interpolated values of \bar{v} at the grid points by many hypothetical independent analysts has a mean which is the true value of \bar{v} at the grid point, so that the entire distribution of the analyst errors has a mean of zero and falls within ± 3 standard deviations. He also represents the error by a one term or linear Taylor series expansion by neglecting higher order terms. Gleeson concludes that the two factors which influence the hand analysis in a region are the average distance between observing stations, and the gradient of the quantity to be analyzed in that region, and shows that:

$$\sigma_a^2 = 0.056 a \left(\frac{\partial \bar{v}}{\partial x} \right)^2$$

$a^{1/2}$ = average distance between stations near the
grid point

$\frac{\partial \bar{v}}{\partial x}$ = gradient of \bar{v} at the grid point where $\frac{\partial \bar{v}}{\partial y} = 0$

The largest values of σ_a^2 occur at 200 mb as did σ_o^2 and σ_m^2 .

This is not unexpected since the highest wind speeds and horizontal wind shears occur at these levels, making measurement and analysis more difficult.

To obtain our reasonable maximum error estimate we will choose the latitude at 200 mb which contains the highest values of σ_a^2 . We can then state that our computed volume of $\sigma[\bar{v}]$ is a reasonable upper limit to the standard error of our zonally averaged meridional

circulation calculations.

The analysis error is greatest in regions of low station density coupled with large \bar{V} gradients. From plotted values of \bar{V} at 200 mb the largest gradients of \bar{V} occur at 30°N latitude where land-sea temperature differences in the extreme seasons set up semi-permanent circulations. For example, from Figure 1.3, 30°N is the approximate boundary of the northward penetration of the Asiatic monsoon.

However, station densities are lowest in the southern hemisphere, especially over the Pacific Ocean. But plotted gradients of \bar{V} in that region are near zero, giving a smaller net value of σ_a^2 than in the Northern Pacific which has a higher station density.

This is not yet conclusive since actual gradients in some low station density regions of the southern hemisphere may be far from zero if broad wind belts go undetected, but our present data is the best available and will be accepted. Therefore we will choose the wind observations at 200 mb and 30°N latitude to compute our upper limit to the standard error of $[\bar{V}]$.

It should also be pointed out that σ_a^2 represents a minimum error distribution and not a true error distribution. Gleeson notes that the use of a truncated Taylor expansion in the derivation results in the elimination of any systematic errors. As mentioned before, in regions of sparse data the distant station spacing may fail to detect a broad region of northerly or southerly winds and result in an important systematic sampling bias and a greatly smoothed gradient of \bar{V} . Citing evidence

from cirrus streaks on satellite pictures, Walker (1969) and Oort et al. (1970) indicate that this may be the case in the central and eastern Pacific. Our upper limit of σ_a^2 may therefore be an underestimate, but it is the best approximation to the analysis error that is presently available.

4.24 Results

Calculations were made for 200 mb and 30°N latitude. Grid point results of the various error quantities are compiled in Table I. Taking a zonal average and estimating $M = 25$ from the plot of station locations in Figure 2, the total error variance becomes:

$$\sigma_{[\bar{v}]}^2 = \left(\frac{.86}{25} + \frac{.28}{25} + \frac{.07}{36} \right) \text{ m}^2/\text{sec}^2$$

$$\sigma_{[\bar{v}]}^2 = .034 + .011 + .002 = .047 \frac{\text{m}^2}{\text{sec}^2}$$

$$\sigma_{[\bar{v}]} = .22 \text{ m/sec}$$

If only σ_a^2 is considered, $\sigma_{[\bar{v}]} = .19 \text{ m/sec}$. This is an upper limit estimate and in general we can conclude:

$$\sigma_{[\bar{v}]} < .20 \text{ m/sec or 95\% confidence limits } \leq \pm 0.4 \text{ m/sec.}$$

For the monsoonal longitudes 40E - 150E and the symmetrical Hadley cell region 160E - 0 - 30E, the number of independent points in the longitudinal average decreases and so the standard error increases. An upper limit error for those meridional velocity calculations are:

40E-150E:

Estimate $M = 9$ from Figure 2

$$\sigma_{\{\bar{v}\}_{MON}}^2 = \frac{1}{9} \left\{ \sigma_a^2 \right\}_{MON} + \frac{1}{9} \left\{ \frac{\sigma_D^2}{N_e} \left(\frac{N_{pe} - N_e}{N_{pe} - 1} \right) \right\}_{MON} + \frac{1}{12} \left\{ \frac{\sigma_m^2}{N} \right\}_{MON}$$

$$\sigma_{\{\bar{v}\}_{MON}}^2 = \left(\frac{.79}{9} + \frac{.33}{9} + \frac{.08}{12} \right) m^2/sec^2$$

$$\sigma_{\{\bar{v}\}_{MON}}^2 = .088 + .037 + .007 = .132 m^2/sec^2$$

$$\sigma_{\{\bar{v}\}_{MON}} = .36 \text{ m/sec or 95\% confidence limits } \leq \pm 0.7 \text{ m/sec}$$

160E-0-30E:

Estimate $M = 16$ from Figure 2

$$\sigma_{\{\bar{v}\}_{HAD}}^2 = \frac{1}{16} \left\{ \sigma_a^2 \right\}_{HAD} + \frac{1}{16} \left\{ \frac{\sigma_D^2}{N_e} \left(\frac{N_{pe} - N_e}{N_{pe} - 1} \right) \right\}_{HAD} + \frac{1}{24} \left\{ \frac{\sigma_m^2}{N} \right\}_{HAD}$$

$$\sigma_{\{\bar{v}\}_{HAD}}^2 = \left(\frac{.89}{16} + \frac{.26}{16} + \frac{.06}{24} \right) m^2/sec^2$$

$$\sigma_{\{\bar{v}\}_{HAD}}^2 = .056 + .016 + .003 = .075 m^2/sec^2$$

$$\sigma_{\{\bar{v}\}_{HAD}} = .27 \text{ m/sec or 95\% confidence limits } \leq \pm 0.5 \text{ m/sec.}$$

Assuming these computed accuracies or confidence limits of ± 0.4 m/sec, ± 0.7 m/sec, and ± 0.5 m/sec for Figures 3.1(a), 3.2(a) and 3.2(b) to be reasonable upper limits we can argue after a cursory examination that the important features such as the direction and relative strengths of the meridional circulations are reliable and at least qualitatively correct.

Before proceeding to the conclusions about our computed meridional circulations, one should note the comparison between this error analysis and the efforts of previous investigators.

The land-sea bias discussed by Walker (1968) is taken into account by the larger analysis error in isolated regions coupled with the realization that belts of unobserved winds may exist in areas of sparse data.

The missing data error is similar to the total error estimate of Oort et al. (1970) with the difference that a finite population representing only the eight years of data was used in our error analysis, resulting in a smaller variance in time of $\sqrt{\quad}$ than Oort calculated, and the complete elimination of his variance in space of $\sqrt{\quad}$.

Finally, the use of the vertical mass average of $[\bar{v}]$ as the indicator of reliability is, of course, encompassed by all three of the errors in our analysis.

Table I

Longitude	N_{AVE}	$\frac{\sigma_D^2}{N_e} \left(\frac{N_{pe} - N_e}{N_{pe} - 1} \right)$	$\frac{\sigma_n^2}{N}$	σ_a^2
180	648	.02	.02	.07
170 ^o W	648	.02	.02	.74
160	697	.01	.02	.41
150	534	.20	.04	.50
140	207	.58	.08	0.00
130	334	.27	.05	.65
120	362	.15	.04	.24
110	401	.09	.04	.96
100	365	.10	.04	.12
90	391	.09	.04	.06
80	404	.12	.04	.06
70	514	.09	.03	.50
60	553	.05	.03	2.50
50	386	.23	.05	4.45
40	250	.62	.07	3.30
30	200	.75	.17	1.23
20	77	.86	.22	.77
10 ^o W	147	.65	.17	.22
0	282	.18	.06	.22
10 ^o E	326	.20	.05	.19
20	348	.14	.05	1.70
30	180	.27	.10	1.70
40	464	.03	.03	.85
50	246	.23	.09	1.40
60	350	.21	.05	1.57
70	363	.12	.05	1.35
80	350	.09	.06	.83
90	90	.96	.18	1.88
100	188	1.04	.15	.62
110	113	.60	.16	.44
120	177	.45	.09	.06
130	419	.09	.04	.14
140	417	.09	.04	.02
150	562	.05	.03	.35
160	429	.26	.05	.77
170 ^o E	477	.24	.05	.06
<u>Averages</u>				
Zonal		.28	.07	.86
40E-150E		.33	.08	.79
160E-0-30E		.26	.06	.89

5. Conclusions and Implications

From a comparison of our averaged meridional circulations presented in Figures 3.1(a), 3.2(a) and 3.2(b) with their respective standard errors, $\sigma_{\overline{V}}$, $\sigma_{\overline{V}}_{MON}$, and $\sigma_{\overline{V}}_{HAD}$, we can conclude that the important gross features of the circulations, even after allowing for these uncertainties, will remain unchanged. Although the calculated mid-tropospheric meridional velocities tend to be smaller than the confidence limits which we can place on them, the upper and lower branches of the monsoonal circulation and the summer and winter hemisphere Hadley cells all retain their direction and strength, even under the worst combination of error corrections possible. This will be shown for the important results of Figure 3.2(b), but can also easily be demonstrated for the two other averaged meridional circulations.

As pointed out in Chapter 4, the computed standard errors represent reasonable upper limits of the true errors in the meridional circulations. In lower latitudes and elevations one would expect the errors to be lower. However, accepting these upper limit error estimates as valid for all latitudes and pressure levels will allow us to examine our calculated values of $\{\overline{V}\}_{HAD}$ in Figure 3.2(b) under more restrictive conditions.

From our value of 0.27 m/sec for $\sigma_{\overline{V}}_{HAD}$ we can say with 95% confidence that our calculated values of $\{\overline{V}\}_{HAD}$ fall within ± 0.5 m/sec of their true value. Discarding any values of $\{\overline{V}\}_{HAD}$ less than 0.5 m/sec, and reducing the absolute value of all other velocities

by 0.5 m/sec would certainly be an overly harsh correction to the calculated circulation. But we can see in Figure 3.2(b) that even if this is done the major flow characteristics would still be unchanged. A summer hemisphere Hadley cell would exist, although somewhat weakened and with a questionable lower branch. Even so, the winter Hadley cell would still penetrate to only 5°N resulting in a nearly symmetrical Hadley cell pattern. Hence one can at least believe in the qualitative results of Chapter 3, and thus the hypothesis has been verified.

It can further be argued that the merging of the rising branches of the summer and winter hemisphere Hadley cells at 5°N during June-August is what would be expected, since from Figure 1.3 this is the approximate position of the ITCZ over the non-monsoonal longitudes.

One can therefore picture the tropical circulation during June-August as containing an intense monsoonal circulation from 40°E - 150°E , with a nearly symmetrical Hadley cell pattern occupying the remaining longitudes. These longitudinal asymmetries, which are the most interesting features of the meridional circulation during June-August, are completely obscured by the zonal averaging process.

Many of the atmospheric transport processes associated with these longitudinal asymmetries may also be overlooked. An example of this is the transport of total angular momentum across the equator during June-August. From the results of Jao (1971) there is a net transport into the northern hemisphere of $12.8 \times 10^{25} \text{ gm cm}^2 / \text{ sec}^2$. However, by taking his data and computing the cross-equator transports for the two

longitudinal sectors we find the following (in units of $\text{gm cm}^2/\text{sec}^2$):

	<u>Monsoon</u> (50E-150E)	<u>Symmetric Hadley</u> (150E-50E)
\curvearrowright -M Transport	-125.9×10^{25}	$+125.9 \times 10^{25}$
Rel. M Transport	<u>10.8×10^{25}</u>	<u>2.0×10^{25}</u>
Total M Transport	-115.1×10^{25}	$+127.9 \times 10^{25}$

Net Transport for all longitudes :

into northern hemisphere: $12.8 \times 10^{25} \text{ gm cm}^2/\text{sec}^2$.

From these results one can see that the monsoon represents a very large net southward mass flux, which is of course exactly balanced by the net northward mass flux of the symmetrical Hadley cell region. This far outweighs the much smaller transport of relative angular momentum which is northward in both regions. Thus although the monsoon accomplishes almost 85% of the net transport of relative angular momentum into the northern hemisphere, it is also responsible for a net transport of total angular momentum into the southern hemisphere during June-August.

These details are obscured in the zonal averages of the momentum transports. Perhaps, as is suggested by Lorenz (1970), future work should deal more with these individual systems and longitudinal asymmetries in the zonal flow field to better understand the processes of the general circulation.

REFERENCES

- Das, P.K., 1968: The Monsoons. National Book Trust, New Delhi, India, 162 pp.
- de Jong, H.M., 1958: Errors in upper-level wind computations. J. Meteor., 15, 131-137.
- Eddy A., 1967: The statistical objective analysis of scale data fields. J. Appl. Meteor., 6, 597-609.
- Gleeson, T.A., 1961: A statistical theory of meteorological measurements and predictions. J. Meteor., 18, 192-197.
- Gordon, A.H., 1953: Seasonal changes in the mean pressure distribution over the world and some inferences about the general circulation. Bull. A.M.S., 34, 357-367.
- Hadley, G., 1735: Concerning the cause of the general trade winds. Philosophical Transactions, 39, 58-62.
- Handbook of Meteorological Instruments, Part II, Instruments for Upper Air Observations, British Met. Office, M.O. 577, London, 1961, 209 pp.
- Jao, Z.-K., 1971: Monsoon and the general circulation of the tropics in June-August. M.S. Thesis, Department of Meteorology, M.I.T.
- Kidson, J.W., 1968: The general circulation of the tropics. Ph. D. Dissertation, Department of Meteorology, M.I.T.
- Kidson, J.W., D.G. Vincent and R.E. Newell, 1969: Observational studies of the general circulation of the tropics: long term mean values. Q.J.R.M.S., 95, 258-287.

- Klein, G. L. , 1968: A comparison of the wind accuracy obtainable from a standard radiosonde and a transponder radiosonde. Instrument Research and Development Report #6, Canadian Meteorological Research Reports, 47 pp.
- Lorenz, E.N. , 1967: The Nature and Theory of the General Circulation of the Atmosphere. World Meteorological Organization, Geneva, 161 pp.
- Lorenz, E.N. , 1970: The nature of the global circulation of the atmosphere: a present view. In The Global Circulation of the Atmosphere, Royal Meteorological Society, London, 3-23.
- Newell, R.E. , J.W. Kidson, D.G. Vincent and G. J. Boer, 1972: The General Circulation of the Tropical Atmosphere and Interaction with Extra-Tropical Latitudes. M. I. T. Press, in press.
- Oort, A.H. and E. M. Rasmusson, 1970: On the annual variation of the monthly mean meridional circulation. Mon. Wea. Rev. , 98, 423-442.
- Spiegel, M. R. , 1961: Theory and Problems of Statistics. Schaum Publishing Co. , New York, 359 pp.
- Starr, V. P. , J.P. Peixoto and N.E. Gaut, 1970: Momentum and zonal kinetic energy balance of the atmosphere from five years of hemispheric data. Tellus, 22, 251-274.
- Stoldt, N. W. , 1971: Effects of missing data on zonal kinetic energy calculations. Pure and Appl. Geoph. , 92, 207-218.
- Walker, H. C. , 1969: Effect of an unbiased grid in determining the kinetic energy balance of the northern hemisphere. M. S. Thesis, Dept. of Meteorology, M. I. T.

Acknowledgements

The author wishes to express his gratitude to Professor Edward N. Lorenz who not only proposed the topic investigated, but, as thesis supervisor, provided continuing assistance and guidance until its completion. Special thanks are due Dr. George Boer who kindly made available the data used in this study, and made many helpful suggestions.

The research was partially supported by the Planetary Circulations Project of Professor V. P. Starr under National Science Foundation Grant No. GA-1310X. Appreciation is extended to Mrs. Barbara Goodwin for typing the manuscript and Miss Isabelle Kole for drafting the figures.